

AD A101741

UNIVERSITY OF CALIFORNIA, BERKELEY

BERKELEY • DAVIS • IRVINE • LOS ANGELES • RIVERSIDE • SAN DIEGO • SAN FRANCISCO

SANTA BARBARA • SANTA CRUZ

SEISMOGRAPHIC STATION  
DEPARTMENT OF GEOLOGY AND GEOPHYSICS

BERKELEY, CALIFORNIA 94720

(11) 26 January 1976

BS

Director, ARPA  
1400 Wilson Boulevard  
Arlington, Virginia 22209

Attn: Program Management

(9) TECHNICAL REPORT NO. 1, 01 DECEMBER 1974 — 30 JUNE 1975

(12) 29

ARPA Order No. 2134  
Program Code 2F10

Contractor: The Regents of the University of California

Effective Date of Contract: 01 December 1974

Contract Termination Date: 30 November 1975

Amount of Contract: \$66,131

Contract No. F44620-75-C-0049

Principal Investigators:

(10) T. V. McEvilly  
(415) 642-4494

L. R. Johnson  
(415) 642-1275

Short Title of Work: NEAR FIELD ACCELEROMETER ARRAY

(15) F44620-75-C-0049  
T. V. McEvilly  
ARPA Order 2134

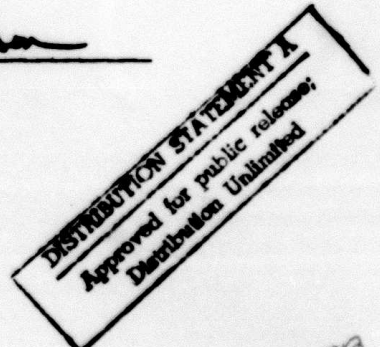
T. V. McEvilly

L. R. Johnson

FILE COPY

Sponsored by  
Advanced Research Projects Agency  
ARPA Order No. 2134

401665



JOB

SECURITY CLASSIFICATION OF THIS PAGE (When Data Entered)

REPORT DOCUMENTATION PAGE		READ INSTRUCTIONS BEFORE COMPLETING FORM	
1. REPORT NUMBER	2. GOVT ACCESSION NO.	3. RECIPIENT'S CATALOG NUMBER	
		<u>AD-A101 741</u>	
4. TITLE (and Subtitle)  NEAR FIELD ACCELEROMETER ARRAY		5. TYPE OF REPORT & PERIOD COVERED  Technical Report 01 Dec 74 - 30 Jun 75	
		6. PERFORMING ORG. REPORT NUMBER	
7. AUTHOR(s)  T. V. McEvilly L. R. Johnson		8. CONTRACT OR GRANT NUMBER(s)  Contract No. F44620-75-c-0049	
9. PERFORMING ORGANIZATION NAME AND ADDRESS  University of California, Berkeley Seismographic Station Berkeley, California 94720		10. PROGRAM ELEMENT, PROJECT, TASK AREA & WORK UNIT NUMBERS  ARPA Order No. 2134 Program Code 2F10	
11. CONTROLLING OFFICE NAME AND ADDRESS  Defense Advanced Research Projects Agency 1400 Wilson Boulevard Arlington, Virginia 22209		12. REPORT DATE  26 Jan 1976	
		13. NUMBER OF PAGES  27	
14. MONITORING AGENCY NAME & ADDRESS (if different from Controlling Office)  Air Force Office of Scientific Research 1400 Wilson Boulevard Arlington, Virginia 22209		15. SECURITY CLASS. (of this report)  UNCLASSIFIED	
		15a. DECLASSIFICATION/DOWNGRADING SCHEDULE	
16. DISTRIBUTION STATEMENT (of this Report)  Approved for public release; distribution unlimited			
17. DISTRIBUTION STATEMENT (of the abstract entered in Block 20, if different from Report)			
18. SUPPLEMENTARY NOTES			
19. KEY WORDS (Continue on reverse side if necessary and identify by block number)  seismology earthquake seismicity earthquake source mechanisms dislocation theory			
20. ABSTRACT (Continue on reverse side if necessary and identify by block number)  This is Technical Report No. 1 for Contract F44630-75-C-0049 and outlines the accomplishments during the period 01 Dec 74 to 30 Jun 75. No changes were made in the near-field accelerometer network during this period. No earthquakes with magnitude greater than 3.0 occurred in the Stone Canyon-Bear Valley region during this report period, and thus no significant additional data were obtained. The general problem of interpreting near-field data in both the time domain and frequency domain is investigated through the use of synthetic seismograms.			

DD FORM 1 JAN 73 EDITION OF 1 NOV 65 IS OBSOLETE

UNCLASSIFIED

SECURITY CLASSIFICATION OF THIS PAGE (When Data Entered)

## TABLE OF CONTENTS

	Page
I. Summary . . . . .	2
II. Technical Data . . . . .	3
III. Earthquake Occurrence Data . . . . .	4
IV. The Interpretation of Near-Field Data . . . . .	6

Accession For	
ETIS	✓
PTC	✓
Unpublished	✓
Justification	
By	
Distribution	
Availability Codes	
Dist:	✓
A	

## I. Summary

The nine stations of the near-field network continue to operate with no changes in either locations or response characteristics. Monitoring of seismic activity in the Stone Canyon-Bear Valley region also is continuing, but no earthquakes occurred during this report period which were of sufficient magnitude to provide good data for the near-field network.

The general problem of interpreting near field data in both the time domain and frequency domain has been investigated through the use of synthetic seismograms. It is shown that within a few source depths of a strike-slip earthquake the static displacements can be significant compared to the dynamic displacements, and this has ramifications in the interpretation of seismic spectra in terms of source parameters. The transverse component of displacement is the least affected and appears to be the component whose spectrum most closely approximates the far-field spectrum of the source time function.

## II. Technical Data

The nine stations of the near-field network have operated in a routine manner throughout the seven months of this report period. The response of the instruments and the configuration of the network have not been changed since May 1974. These characteristics can be found in Figures 1 and 3 and Table 2 in the Final Report, AFOSR Grant No. 72-2392, 15 May 1975.

Our main problems have been concerned with keeping the air conditioners and tape recorders in the old LRSM vans in operation. The air conditioner in one of the vans is now beyond repair, so most of the critical equipment is now operated in the other van which has an operating air conditioner. Failures of the old Ampex tape recorders are becoming more frequent and spare parts more difficult to obtain. However, in spite of these problems, no significant data have been lost during this report period.

USGS has announced plans for downgrading Stone Canyon Observatory on 30 June 1975. This will have some effect upon our operation and we are considering various alternatives now. One attractive possibility is to record all of the network data in direct-record fashion on a single tape recorder in the concrete block building. However, this will require the purchase or lease of a new 15/16 ips tape transport.

### III. Earthquake Occurrence Data

Table 1 gives the hypocentral data for events in the Bear Valley-Stone Canyon area with  $M_L$  2.5 or greater for the period 9/9/74 through 9/20/75. The first two events in the table overlap with Table 1 in Section III of Technical Report No. 4, AFOSR Grant No. 72-2392, 10 November 1974. This is because the first event in the current table is a slightly revised hypocenter of the event in the earlier report. As can be seen in Table 1, none of the events in this report period had magnitudes greater than 3.0 and thus none of them were a source of good data for the near-field accelerometer network.

Table 2. Bear Valley - Stone Canyon earthquakes with  $M_L$  2.5 and greater.

<u>Event</u>	<u>Origin Time</u>	<u>Latitude</u>	<u>Longitude</u>	<u>Depth</u>	<u>Magnitude</u>
<u>Date</u>	<u>Time</u>				
09-09-74	0248	3641.8	12120.7	2.50	2.5
09-12-74	2121	3638.0	12115.1	6.21	3.0
11-14-74	2301	3640.5	12118.6	4.32	2.8
02-20-75	0515	3636.0	12112.8	7.17	2.5
02-23-75	1724	3634.3	12110.3	4.96	2.7
03-26-75	2013	3638.90	12116.40	3.83	3.1
05-23-75	0516	3640.00	12118.00	2.28	2.5
06-14-75	1256	3640.80	12119.30	3.75	3.0
07-04-75	1932	3634.60	12102.70	8.48	2.7
08-11-75	1103	3634.12	12105.04	7.05	2.5
08-27-75	0953	3638.86	12116.47	4.12	2.5
08-31-75	0552	3632.98	12108.77	7.23	2.8
09-06-75	0517	3635.07	12107.69	8.43	2.7
09-20-75	0051	3633.06	12106.26	8.36	2.6

#### IV. The Interpretation of Near-Field Seismic Data

Earthquakes are generally acknowledged to be complicated events that derive their peculiar properties from a complex interaction of tectonic stresses, material properties, and failure criteria all compounded by the inhomogeneity of the earth in which they occur. The problem is further complicated by the fact that in practically all cases we must study the earthquake source indirectly through the elastic waves that it generates, and the propagation of these elastic waves is itself a difficult and not completely solved problem. Thus it is not difficult to understand why the search for a mathematical model which satisfactorily simulates the earthquake process has been a difficult one, and why a considerable number of approximations and simplifications have usually been necessary in such studies. However, in the face of this rather pessimistic prognosis, it is encouraging to note that one such theoretical model, that of representing an earthquake as a dislocation, has proved moderately successful in simulating some of the gross observational properties of earthquakes. The elasticity theory of dislocations is essentially mathematical in nature and is obviously incomplete in that it ignores practically all of the physical processes associated with the earthquake source. On the other hand, the simplicity of this theory does have the advantage of being very tractable for various types of computational experiments.

The concept of an earthquake as being due to the relative movement of two faces of a fault, which grew out of the observation of surface faulting accompanying some earthquakes and the success of the fault plane solution method in explaining the polarity of radiated seismic waves, led Vvendenskaya

(1956, 1959) and Steketee (1958a, 1958b) to suggest dislocation theory as an appropriate mathematical model for an earthquake. Incorporating this dislocation theory into an elastic representation theorem (Knopoff, 1956; DeHoop, 1958) leads to a simple and elegant mathematical model of an earthquake source. Studies of the dynamic problem employing this general approach include the early studies of Knopoff and Gilbert (1959, 1960), Maruyama (1963), Haskell (1964, 1966, 1969), Burridge and Knopoff (1964), and Aki (1967) and numerous more recent papers.

The general objective of the research project which this contract supports is to collect and interpret seismic data very near to an earthquake. To date, nature has not provided enough earthquakes of sufficient magnitude within the near-field network in order to acquire the necessary data set to complete the project, but considerable effort has gone into the consideration of how such data should be analyzed. In the present endeavor, we adopt a simple dislocation model of an earthquake source and then proceed to investigate the types of waves that would be recorded at near distances and if and how useful information about the source can be extracted from the analysis of these waves.

Most previous studies have included only the far-field terms of the solution and thus obtain solutions which are valid only beyond a certain distance from the source. In the present study we use an exact formulation including near-field terms (Johnson, 1974) and attempt to evaluate the relative effects of the near-field terms. A second common simplification is to consider the source to be imbedded in an infinite space; when the free surface of the earth is taken into account it is done in an approximate manner.

The present study will use an exact formulation for a homogeneous half-space so that the appropriateness of these approximate methods can be evaluated.

As mentioned above, an objective of the present study is to investigate methods which can be used to interpret observational data collected relatively near to an earthquake. Many of the parameters which have recently become popular as a means of characterising the earthquake source, such as spectral estimates of moment and corner frequencies, are implicitly dependent upon obtaining the spectrum of a single far-field body wave pulse. This type of analysis is considerably complicated when applied to data recorded very near the source and it remains to be shown that meaningful estimates of source parameters can still be extracted from the calculated spectra.

As the purpose of this study is to investigate ground motions in the near-field of a dislocation model of an earthquake, the concept of 'near-field' should first be defined. As used here, the near-field part of the elastic wave solution is taken to be those terms whose amplitudes attenuate with inverse distance raised to a power greater than 1. In contrast, the far-field part is those terms whose amplitudes attenuate with inverse distance raised to the first power. The 'near-field' is thus defined as the region around the source where the near-field part of the solution is comparable in magnitude with the far-field part. To be more precise, the amplitudes we are considering here are actually the spectral density amplitudes, and thus 'near-field' is a frequency dependent concept. In a practical sense, the near-field is that region within a few wavelengths of the source. We note in passing that the 'near-field' is sometimes defined to be that region within a few source dimensions of the source, but

this concept will not be used here because we will only be considering point sources.

It is also worth mentioning at the outset some of the advantages and disadvantages of working with data recorded in the near-field, starting with the advantages. One would expect that the propagation effects which must always be removed from observed data before the source can be studied, would increase with distance from the source. For instance, in studying near field data of shallow earthquakes, the presence of the mantle can effectively be ignored. In general, the attenuation due to imperfect elasticity which is generally characterized by the seismic quality factor Q, is poorly known and its effects increase with propagation distance. Thus, by making observations close to the source the uncertainty introduced by this ignorance is minimized. Another problem which plagues the interpretation of data observed in the far-field is that the finite duration of the source is inextricably combined with the finite dimensions of the source. In the near-field there exists at least the possibility that these two effects can be separated.

Naturally, there are also problems associated with recording and analyzing data in the near-field. A primary one involves the fact that the individual seismic pulses appear on the seismogram separated by intervals that are often less than the duration of the pulses. This makes it difficult to isolate and study a particular pulse. Another problem is that the various types of near and far field phases emanating from the source reflect its time history in different manners. The permanent displacements, tilts, and transient pulses all radiate from the same source and their effects are combined on the seismogram.

The geometry employed for the calculations of this study is illustrated in Figure 1. A strike slip earthquake is simulated by a point dislocation on a vertical plane at a depth of  $h=4$  km within a homogeneous halfspace. The elastic halfspace is taken to have a compressional velocity of 5.4 km/sec, a shear velocity of 2.89 km/sec, and a density of  $2.67 \text{ gm/cm}^3$ . On the surface at various epicentral distances  $\Delta$  and azimuths  $\phi$  three orthogonal components of ground displacement, radial R, transverse T, and vertical Z, are calculated as a function of time. The displacements are calculated at distinct time points separated by intervals of 0.002 sec and then connected by linear interpolation. The mathematical formulae for these calculations are all given in Johnson (1974). The static displacements were checked by reformulating for an arbitrary elastic medium the results of Maruyama (1964).

Note that the assumption of a point source is strictly valid only when the actual source dimensions are small compared to both a wavelength and the distance between source and receiver. The method employed in this paper can readily be extended to the case of finite propagating dislocations over finite source areas, but it seems that a study of this type would be premature before the basic effects of a point source are properly understood.

The time history assumed for the dislocation source is basically a step in displacement with a finite rise time. The function assumed throughout this study along with its first time derivative and the spectra of both are shown in Figure 2. The rise time is 1 sec. This particular function was proposed by Litehiser (1976) and has the property that the function and its first two time derivatives are all continuous. This means that the

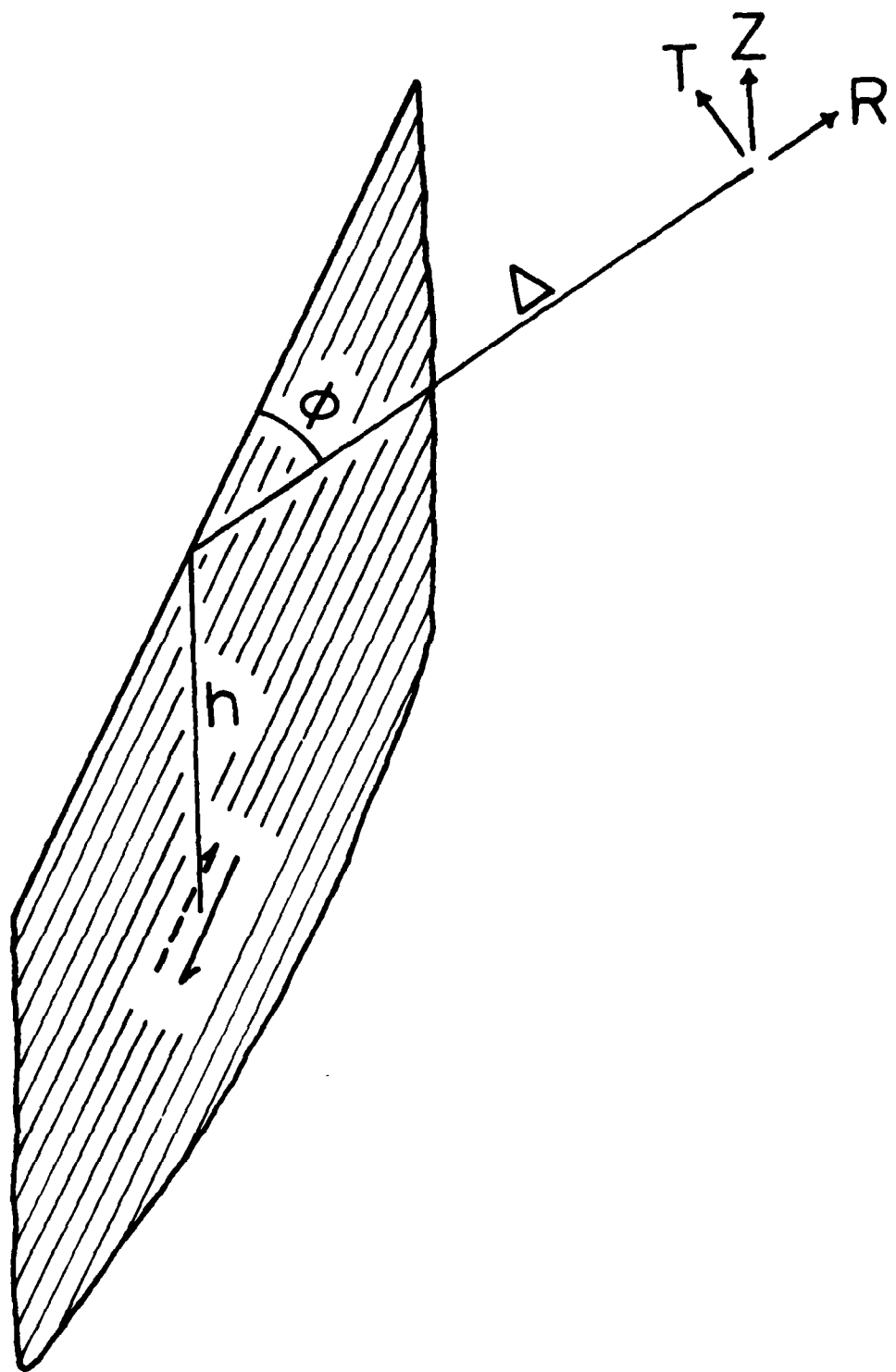


Figure 1. Geometrical relation between the point strike-slip dislocation source and the point on the the surface of the half-space where three components of displacement, R, T, and Z, are calculated.

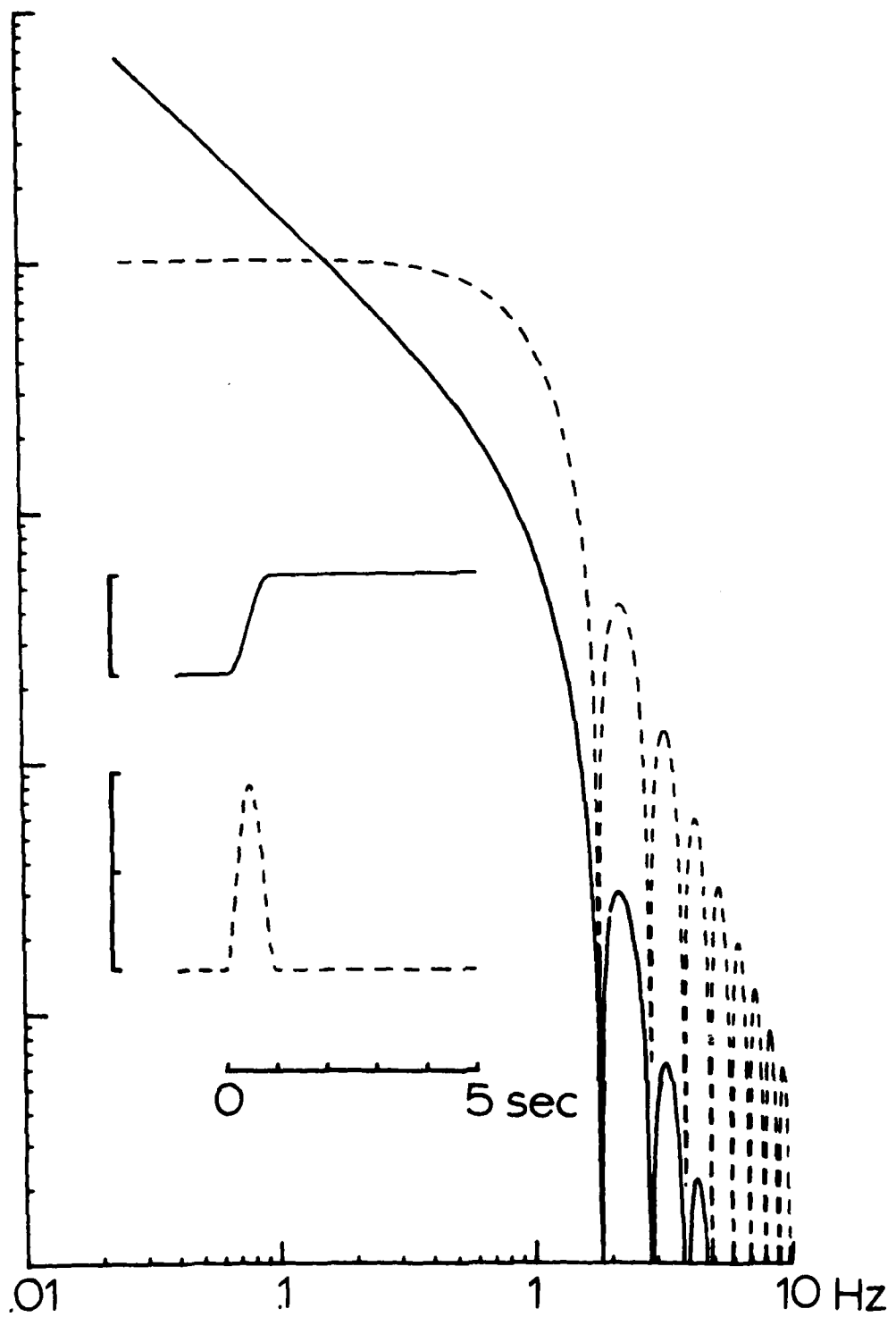


Figure 2. Time function and spectrum of the dislocation source (solid line) and corresponding graphs for its first time derivative (dashed line) which is the equivalent far-field source function.

the spectra of the far-field pulses (first derivative of the source function) fall off as inverse frequency to the third power at high frequency. Note that the corner frequency of this far-field pulse, taken as the intersection of the asymptotes to the high and low frequency parts of the spectrum, is at 1 Hz, the inverse of the rise time. Also note that the whole spectrum of the far-field pulse is flat at low frequencies, but the spectrum of the near-field pulses (which are more closely related to the actual source function instead of its first derivative) will have a slope approaching the inverse frequency to the first power at low frequencies.

Let us now calculate ground displacement as a function of epicentral distance and azimuth for the source model just described. As mentioned earlier, it is convenient to consider the radial ( $R$ , positive away from the source), transverse ( $T$ , positive counterclockwise about the source), and vertical ( $Z$ , positive upward) components of displacement at each point. It is easy to show that for a strike-slip point dislocation source on a vertical fault plane, the dependence upon the azimuth  $\phi$  enters the radial and vertical components as  $\sin(2\phi)$  and enters the transverse component as  $\cos(2\phi)$ . With such symmetry it is only necessary to consider the solution in the azimuthal range of 0 to  $\pi/4$ . This symmetry holds for both near and far-field parts of the solution.

Figure 3 shows ground displacement calculated for a point strike-slip dislocation source at four distinct azimuths and five distances. To a first approximation, the character of the seismograms depends primarily upon the ratio of horizontal distance to source depth, which varies between 0.5 and 8 in this figure, and thus these results can also be used to infer the general nature of ground motion for other source depths.

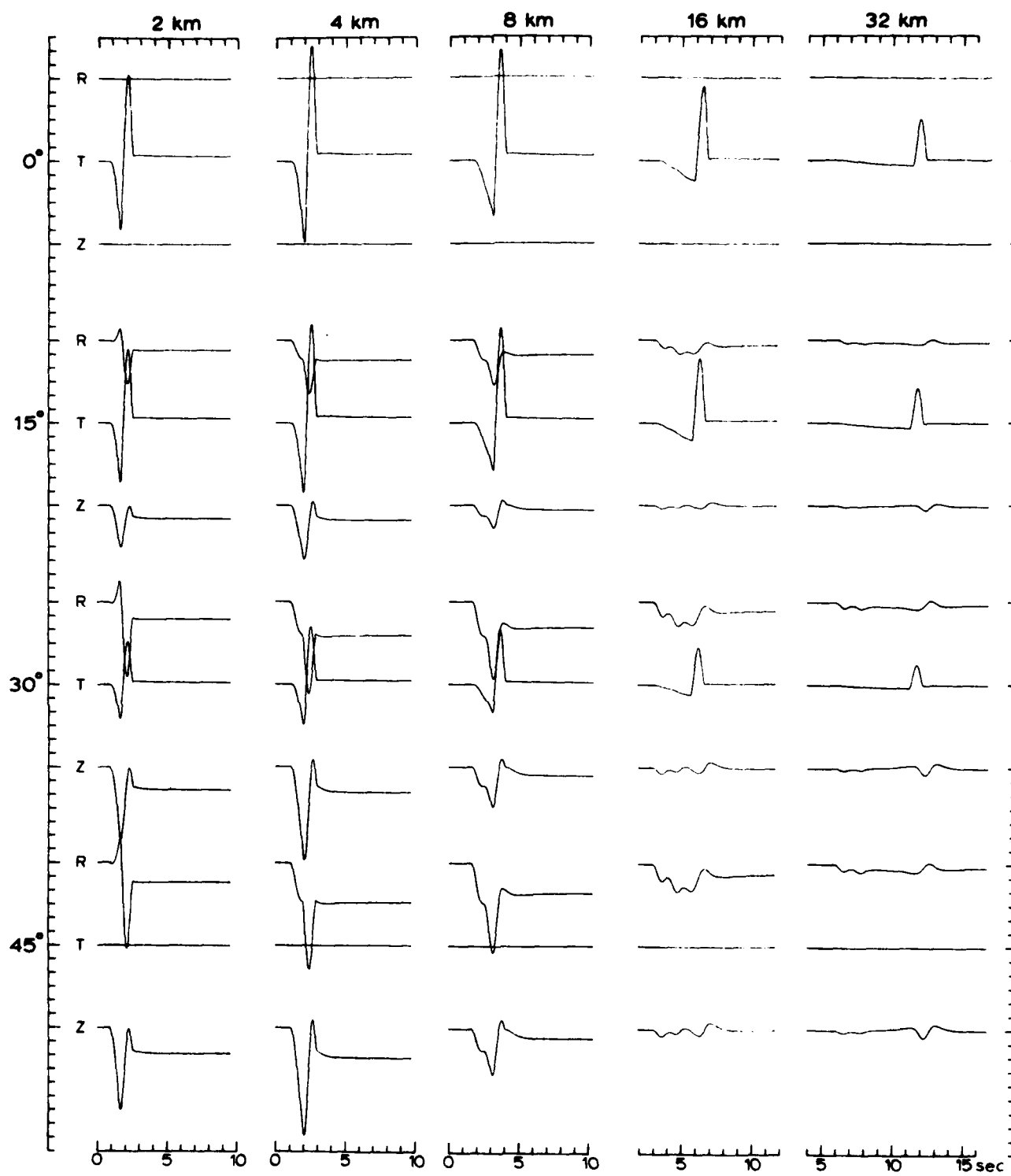


Figure 3. Radial (R), transverse (T), and vertical (Z) components of ground displacement as a function of distance (from left to right) and azimuth (from top to bottom) from a strike-slip dislocation source at a depth of 4 km. For a source moment of  $2.23 \times 10^{24}$  dyne-cm, each division on the vertical scale corresponds to 1 cm of ground displacement.

The following features of the ground motions displayed in Figure 3 are worth pointing out:

- a) The azimuthal radiation patterns pointed out above are obvious in this figure. Thus, the transverse component is maximum along the strike of the fault and has a null at an azimuth of  $\pi/4$ , while the radial and transverse components obey a converse relationship. The form of the displacements does not change as a function of azimuth; only the amplitude is affected.
- b) The near-field parts of the solution are apparent in several ways. The static displacements, which are entirely due to the near field parts, can be a significant fraction of the maximum dynamic displacements, for example, in the case of the R component in the distance range of one or two source depths. The motion on all components begins with the arrival of the P wave. On the T component this means that all motion between the arrival of the P and S waves is due entirely to near-field parts of the solution, and this motion can be quite large and is significant out to distances of at least four source depths. On the R and Z components it is not so easy to identify the near and far-field parts of the motion.
- c) At all distances greater than about one source depth the diffracted sP phase plays a prominent role on the R and Z components of motion. It arrives between the P and S wave and its amplitude can be as large as that of the P wave.

The ground displacements shown in Figure 3 were calculated for a source moment of  $2.23 \times 10^{24}$  dyne cm. Using the empirical moment-magnitude results of Johnson and McEvilly (1974) for central California earthquakes,

these displacements would be appropriate for an earthquake with  $M_L = 5.8$ . In Figure 4 the ground displacements of Figure 3 have been passed through the response of a Wood-Anderson torsion seismograph system. A gain factor of 1 was used in this calculation, so, in terms of the standard Wood-Anderson system with a magnification of 2800, Figure 4 represents the seismograms from an  $M_L = 2.3$  earthquake. If one applies the standard method of Richter (1958) and computes  $M_L$  from these synthetic seismograms, one gets a value of about 1.6. This difference could have many causes, the most likely being the fact that low velocity materials which usually are present near the surface and which amplify and prolong the motion on the seismograms have not been included in our theoretical formulation of the problem.

A common method of inferring the characteristics of a seismic source is through the interpretation of a spectrum computed from a seismogram. The procedure for doing this is reasonably well-justified when dealing with far-field body wave pulses, but in the present study we wish to investigate whether similar methods can be applied to data obtained relatively near the source. In doing this, it is first necessary to appreciate a couple of additional problems that arise in the process of estimating spectra from seismograms recorded in the near-field.

Examination of Figure 3 shows that the seismogram does not consist of distinct and separate pulses such that the spectrum can be calculated for an individual pulse. Addition of the effects of an instrument, such as in Figure 4, further blurs the distinction between individual pulses. In this situation about the only recourse, and the one followed here, is to calculate the spectrum of the entire seismogram. It then remains to be

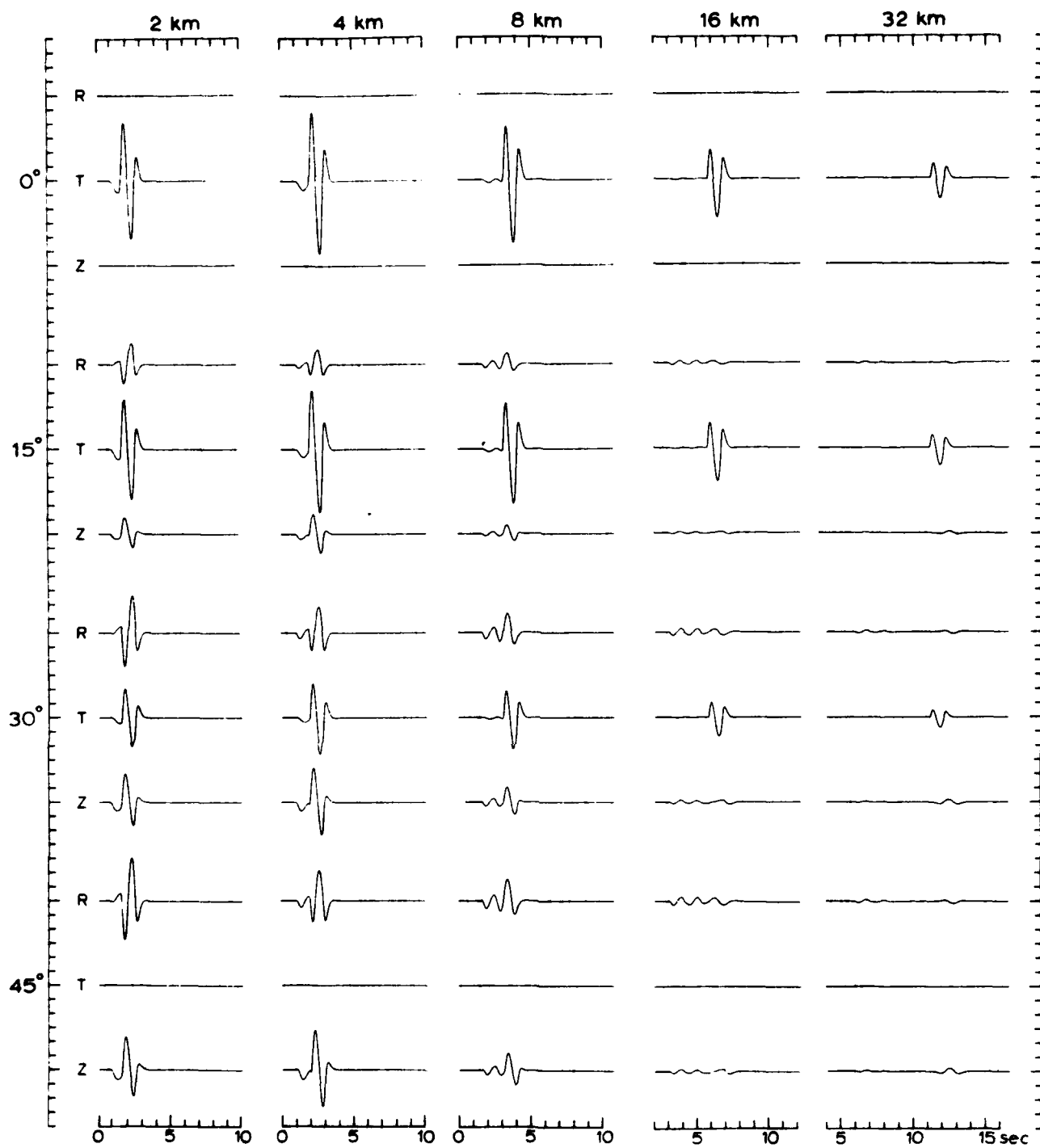


Figure 4. Outputs from a Wood-Anderson torsion seismograph for the ground displacements shown in Figure 3. For an earthquake of  $M_L = 2.3$ , each division on the vertical scale corresponds to 1 cm of displacement on the seismogram.

shown that useful information about the source can still be extracted from such 'whole-record' spectra.

The analytical procedure used in estimating the spectrum also becomes more critical when dealing with near-field data. In this, as in most other studies of this type, the spectrum is interpreted to be an estimate of the Fourier transform, which is consistent with assuming that earthquakes are transient phenomena. The finite Fourier transform, in particular the Cooley-Tukey algorithm, is usually used in the estimation process. In cases where the time trace actually is a transient event which is contained within the time window being analyzed, the finite Fourier transform does provide a legitimate estimate of the Fourier transform. In the far field this situation can usually be assured by making the time window long enough to include the duration of the significant ground motion of a particular pulse plus the duration of the instrument response function. However, in cases where the time trace suffers a constant offset in the course of an earthquake it can not be considered a transient event, and the finite Fourier transform will not correctly estimate the Fourier transform. Such a situation is a definite possibility when using instruments which have a dc response or a tilt response. It is also clear that this situation exists with the records of ground displacement shown in Figure 3. There are different methods of avoiding the spectral estimation problem mentioned above, but the approach followed here was to differentiate the time trace before transforming it (thus converting any step that it contains into a transient) and then removing the effect of the differentiation in the frequency domain.

Figures 5, 6 and 7 show the amplitude density spectra estimated from the ground displacements of Figure 3 for the R, T, and Z components of displacement, respectively. Again, as in the case of Figure 3, the effect of azimuth is only to change the amplitude. As a general comment, there is a considerable variation in this suite of spectra from the same source. The spectra estimated from the T component (Figure 6) show the most similarity to the spectrum of the far-field spectrum of the source (Figure 2), and thus would probably be most useful in estimating such source parameters as rise time and moment. This result could have been anticipated from Figure 3 where we see that the relative size of the static part of the solution is minimum on the T component. On the other components, particularly that of R in Figure 5, the process of estimating moment from the flat low-frequency portion of the spectrum is made difficult by the static near-field parts of the solution which produce a  $1/f$  dependence at low frequencies. This feature also interferes to a certain extent with the estimation of the corner frequency of the spectrum. It is also obvious, say, on the T and Z components of Figure 6 and 7, that interference effects can result in a peaked spectrum even when the far-field source spectrum (Figure 2) is not peaked.

So far our analysis has indicated that at least one portion of the near-field part of the solution for a strike-slip dislocation source, the static displacement, can be significant for data recorded relatively near the source. The relationship between maximum dynamic and static displacements for a strike-slip source at a depth of 4 km and the source time function of Figure 2 is shown in Figure 8. Note that the static displacement can be as much as half of the peak dynamic displacement, for instance on

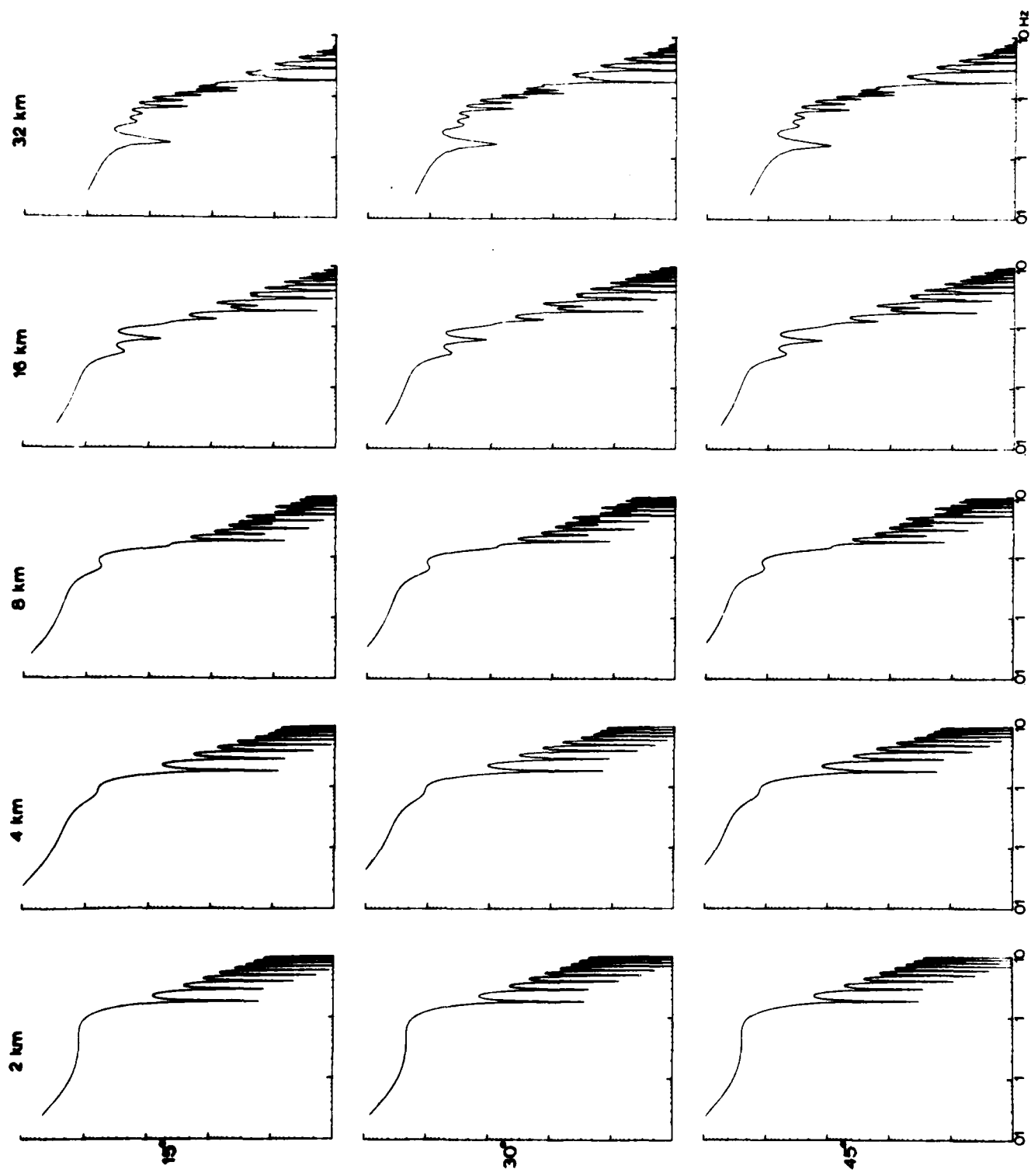


Figure 5. Amplitude density spectra of the ground displacements of the R components shown in Figure 3.

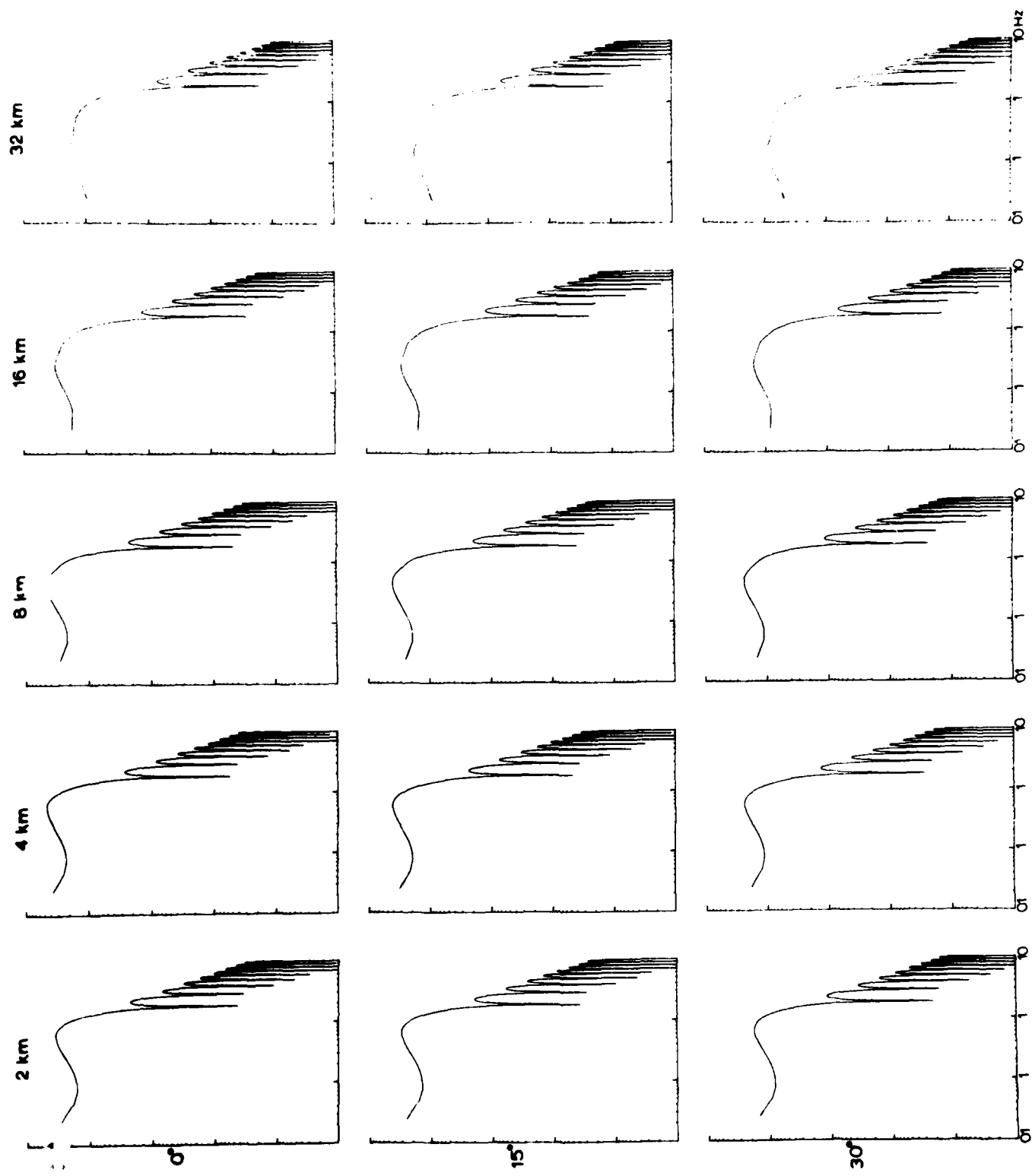


Figure 6. Amplitude density spectra of the ground displacements of the T components shown in Figure 3.

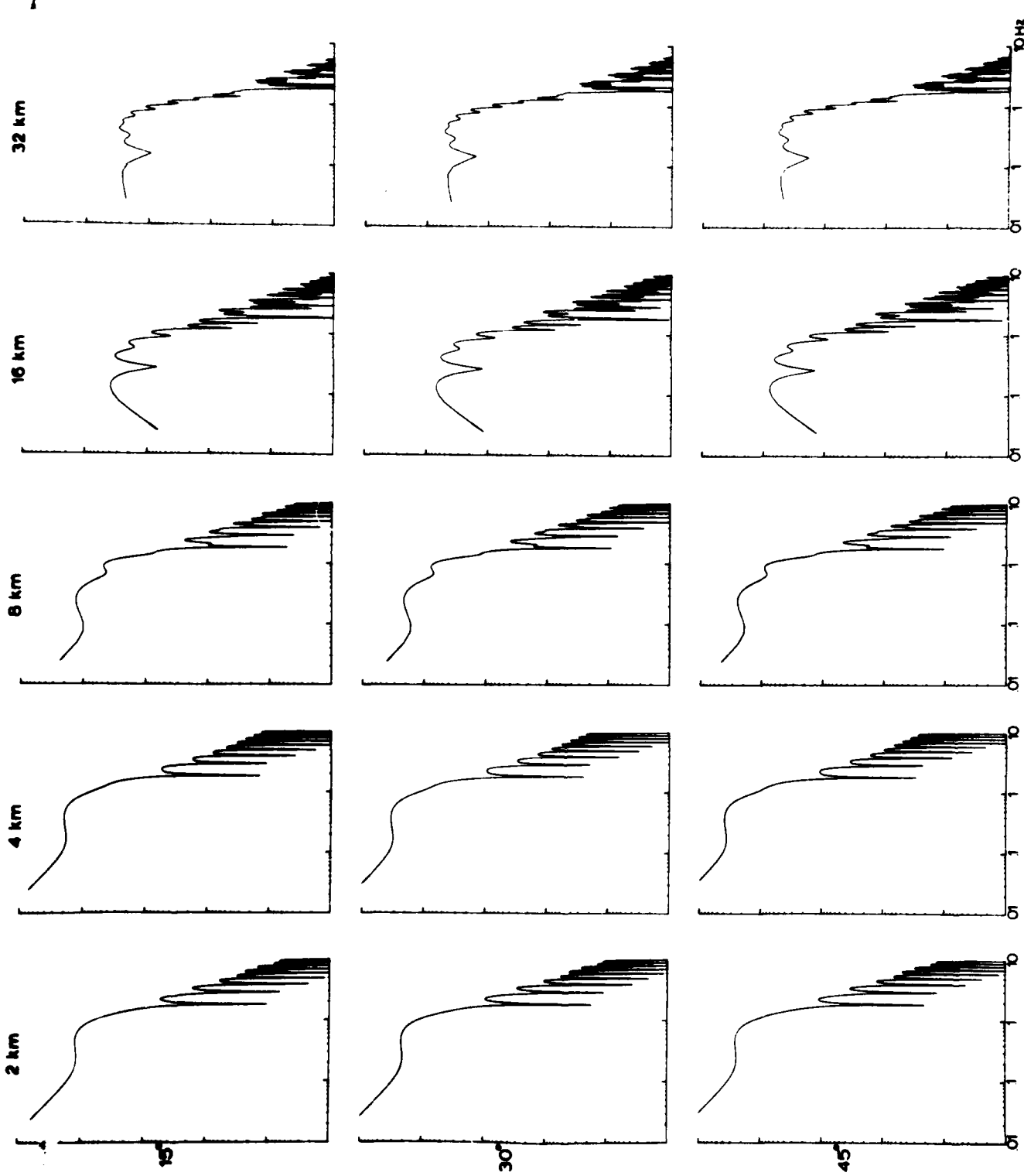


Figure 7. Amplitude density spectra of the ground displacements of the Z components shown in Figure 3.

the R component, and that, surprisingly, this can occur at distances of several source depths.

Finally, let us consider the effect of the free surface upon the ground displacements produced by a strike-slip source. In Figure 9 we have a comparison between the half space solution such as given in Figure 3 and a displacement obtained by computing the whole space solution and multiplying it by 2 as an approximation to the free surface effect. At small distances, the differences between the two solutions are minor, and for the T component this holds at all distances. However, for the R and Z components at larger distances, the presence of the sP and Rayleigh phases in the half space solution begin to cause significant differences. For instance, for the Z component at 16 km the polarities of the two solutions are not even the same for much of the record. The differences in the spectra follow the same trend, being minimum on the T component and maximum on the Z component.

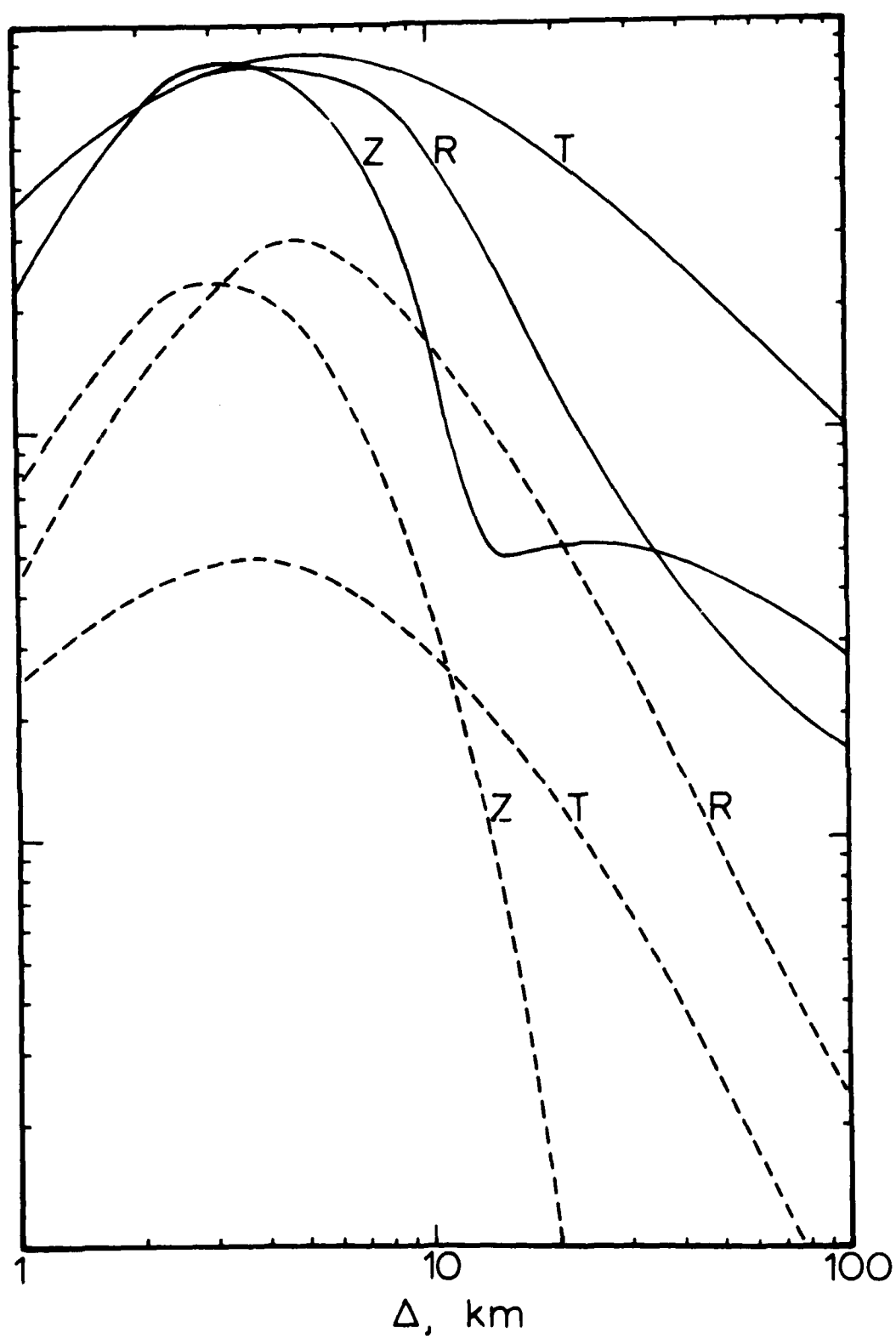


Figure 8. Maximum dynamic displacements (solid line) and final static displacements (dashed line) for the ground displacements shown in Figure 3.

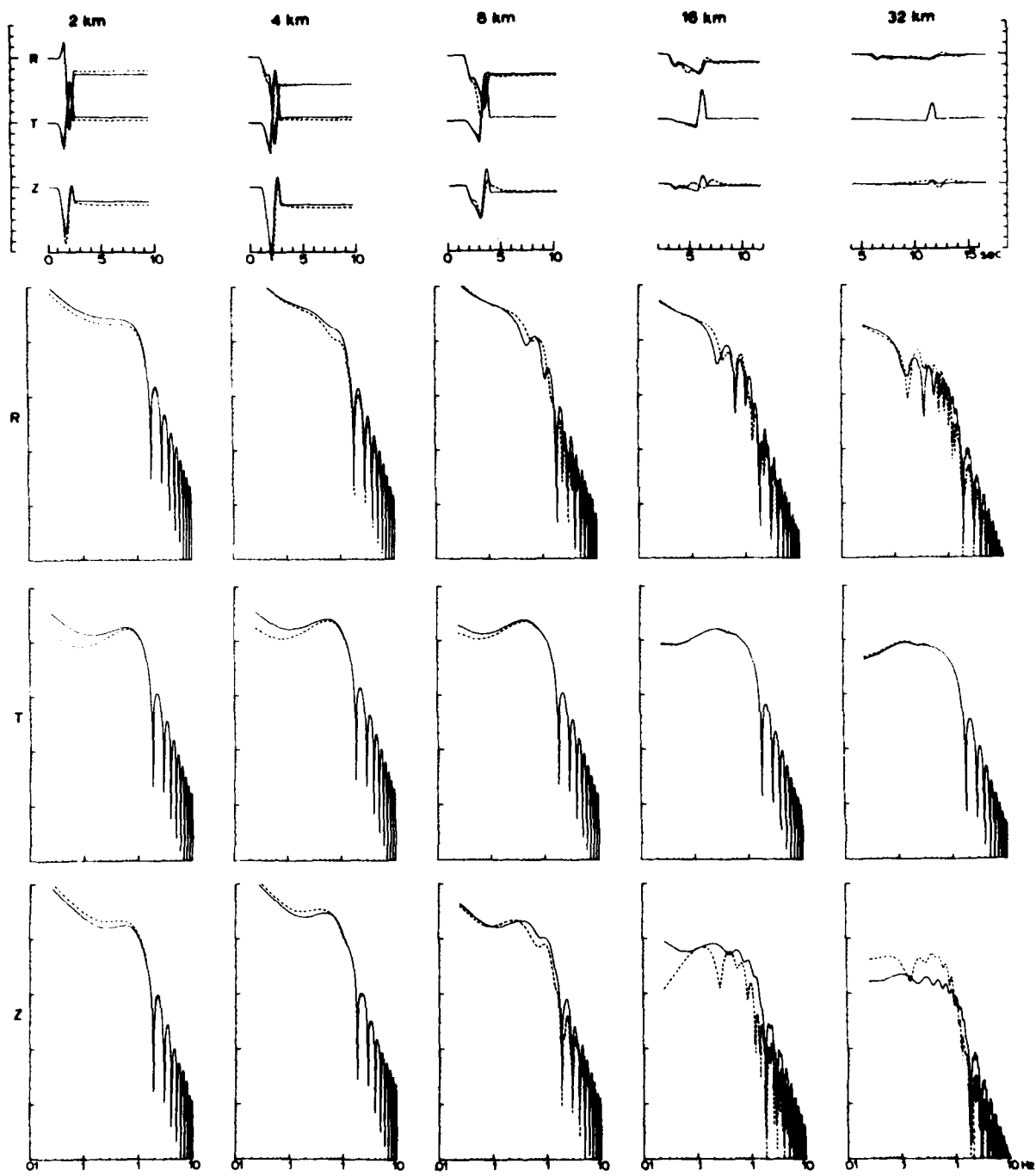


Figure 9. Comparison between the whole-space solution (solid line) and the half-space solution (dashed line) for the same source as in Figure 3 and an azimuth of  $30^\circ$ .

## References

Aki, K., Scaling law of seismic spectrum, J. Geophys. Res., 72, 1217-1231, 1967.

Burridge, Knopoff, L., Body force equivalents for seismic dislocations, Bull. Seism. Soc. Am., 54, 1875-1888, 1964.

DeHoop, A. T., Representation theorems for the displacement in an elastic solid and their application to elastodynamic diffraction theory, Thesis, Delft, Netherlands 83 p, 1958.

Haskell, N.A., Total energy and energy spectral density of elastic wave radiation from propagating faults, Bull. Seism. Soc. Am., 54, 1811-1841, 1964.

Haskell, N. A., Total energy and energy spectral density of elastic wave radiation from propagating faults, Part II, A statistical source model, Bull. Seism. Soc. Am., 56, 124-140, 1966.

Haskell, N. A., Elastic displacements in the near-field of a propagating fault, Bull. Seism. Soc. Am., 59, 865-908, 1969.

Johnson, L. R., Green's function for Lamb's problem, Geophys. J. R. Astr. Soc., 37, 99-131, 1974.

Johnson, L. R. and McEvilly, T. V., Near-field observations and source parameters of central California earthquakes, Bull. Seism. Soc. Am., 64, 1855-1866, 1974.

Knopoff, L., Diffraction of elastic waves, J. Acoust. Soc. Am., 28, 217-229, 1956.

Knopoff, L. and Gilbert, F., First motion methods in theoretical seismology, J. Acoust. Soc. Am., 31, 1161-1168, 1959.

Knopoff, L. and Gilbert, F., First motions from seismic sources, Bull. Seism. Soc. Am., 50, 117-134, 1960.

Litehiser, J. J., Near-field seismograms from a propagating two-dimensional dislocation, Ph.D. Thesis, University of California, Berkeley, 1976.

Maruyama, T., On the force equivalents of dynamical elastic dislocations with reference to the earthquake mechanism, Bull. Earthquake Res. Inst., 41, 467-486, 1963.

Maruyama, T., Statical elastic dislocations in an infinite and semi-infinite medium, Bull. Earthquake Res. Inst., 42, 289-368, 1964.

Richter, C. F., Elementary Seismology, W. H. Freeman and Co., 768 p, 1968.

Steketee, J. A., On Volterra's dislocations in a semi-infinite elastic medium, Can.J. Phys., 36, 192-205, 1958a.

Steketee, J. A., Some geophysical applications of the elasticity theory of dislocations, Can.J. Phys., 36, 1168-1198, 1958b.

Vvedenskaya, A. V., The determination of displacement fields by means of dislocation theory, Izvestia, Geophys. Ser., 227, 1956.

Vvedenskaya, A. V., The displacement field associated with discontinuities in an elastic medium, Izvestia, Geophys. Ser., 516-526, 1959.